ChemComm

COMMUNICATION

View Article Online
View Journal | View Issue

Cite this: *Chem. Commun.*, 2023, **59**, 1505

Received 15th December 2022,
Accepted 13th January 2023

DOI: 10.1039/d2cc06843e

rsc.li/chemcomm

Growth of chemical gardens in gaseous acidic atmospheres†

Georgios Angelis,[a] Georgios Sant,[a] Ioannis S. Vizirianakis[ab] and Georgios Pampalakis*[a]

The generation of chemobrionic architectures through slow injection of aqueous silicate solution in gaseous $TiCl_4$ is demonstrated. The tubes were characterized by XRD, SEM and wet chemistry control experiments, and their mechanism of formation was unraveled. These structures serve as laboratory models for calthemites or soda straws.

Chemical gardens were initially described in 1646 and constitute hollow plant-like structures that develop upon addition of a metal salt (seed) in a solution of silicates.[1] Within the last years, the growth of chemical gardens in other than silicates such as borates, phosphates, and carbonates,[2] in organic media,[3] in only hydroxide solution,[4] or even in natural silica rich spring waters[5] has been described. The formation of chemical gardens is characterized by a complex mechanism of growth that involves osmosis, buoyancy, and reaction–diffusion processes.[6] The field that studies chemical gardens and related phenomena based on out-of-equilibrium self-assembly was coined chemobrionics.[2] Many current chemical garden experiments are conducted using flow-injection systems that provide uniform and convenient control of the reactions.[7]

Chemical gardens constitute laboratory analogs of hydrothermal vents, the places where life has been suggested to emerge approximately 4 billion years ago.[8] Therefore, the study of chemical gardens is also of astrobiological significance. In this direction, it was shown that chemical garden can grow in solutions that simulate the Enceladus' Ocean.[9] Further, study of chemical gardens has applications in metal corrosion,[10] in cement chemistry[11] but it also has biomedical applications that include drug delivery systems[12] and cellular scaffolds.[13] Recently the calcium phosphate chemical gardens were suggested as new bone substitute materials.[14]

In 2004, the generation of a chemical garden through injection of ferrous sulfate in H_2S or NH_3 atmosphere was reported but not studied further.[10] These structures externally resemble the soda straw stalactites, nonetheless the mechanism of soda straw formation is different from chemical gardens and involves CO_2 degassing.[15]

Here, we initially investigated the potential to form chemical gardens in a gaseous atmosphere using the system Na_2SiO_3/$TiCl_4$. For this, injection of sodium silicate (composition of stock solution: SiO_2/Na_2O ratio 3.34; SiO_2 27.99%; Solids 36.66%) was performed in an argon purged glass chamber saturated with $TiCl_4$ vapor. In this mode, the chemobrionic structures are growing in a reverse manner, that is injection of the silicate in the metal containing chamber, but also in an inverted manner since they grow in the same direction with gravity (Fig. 1). The growth was monitored under different injection flow rates.

The chemobrionic structures were removed, washed with distilled water, allowed to dry in a Petri dish, powdered, and

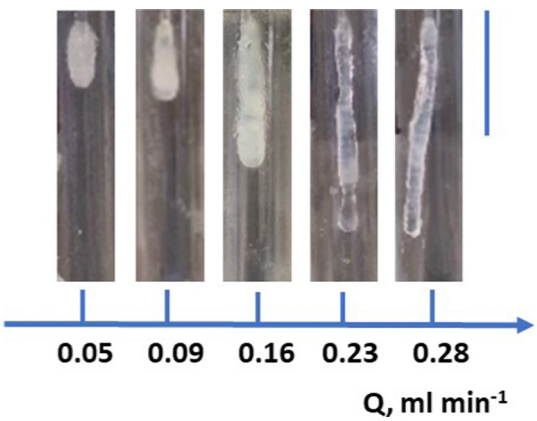

Fig. 1 Experimental growth of chemical gardens in $TiCl_4$ gaseous atmospheres. All pictures shown were obtained for the same time of growth. As expected, the length depends on the flow rate, *Q*. The scale bar on the right corresponds to 4 cm.

[a] *Laboratory of Pharmacology, School of Pharmacy, Aristotle University of Thessaloniki, Thessaloniki, 54124, Greece. E-mail: gpampalakis@pharm.auth.gr*
[b] *Department of Life and Health Sciences, University of Nicosia, Nicosia 2417, Cyprus*

† Electronic supplementary information (ESI) available. See DOI: https://doi.org/10.1039/d2cc06843e

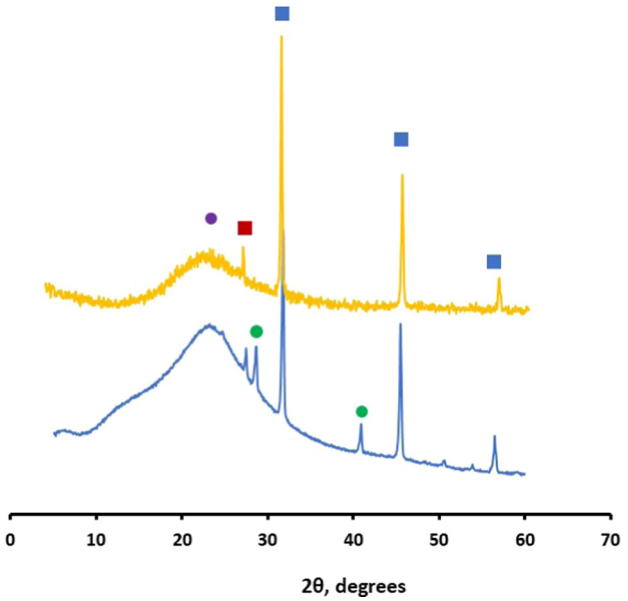

Fig. 2 X-Ray diffraction analysis of the chemobrionic structures grow in $TiCl_4$ (blue) and HCl (dark yellow) atmosphere. X-Ray powder diffraction (Rigaku-MiniFlex II, Chalgrove, Oxford, UK) was obtained with CuKa radiation for crystalline phase identification. The sample was scanned with a speed of 1° min^{-1}. The peaks labelled with blue squares indicate halite, the broad peak labelled with purple circle indicates SiO_2, the green circles indicate the rutile, while the peak labelled with dark red square probably indicates sodium silicate. Details are shown in text.

analyzed with X-ray diffraction (XRD) as shown in Fig. 2. It can readily be observed that the tubular structure is mainly composed of silicon oxide. Specifically, the broad peak at 2θ = 23° is due to amorphous SiO_2 while the peaks at 2θ = 31.75°, 45.50°, and 56.5° are due to halite (NaCl) that is the byproduct of the reaction. Probably, the halite has been incorporated into the chemobrionic structure and thus was not removed during the washing step. The peaks at 28.65° and 40.90° probably indicate rutile (TiO_2) [110] and rutile [111], the product of $TiCl_4$ hydrolysis, since these peaks are absent in the diffractogram obtained from the sample grown in HCl atmosphere (described in the next paragraph). The peak at 27.45° that is observed in both $TiCl_4$ and HCl samples is probably a form of sodium silicate.

The silicon oxide is likely produced upon reaction of the gaseous $TiCl_4$ with the water present in the injected aqueous silicate solution. This yields TiO_2 and HCl. The acid further reacts with silicates to produce and deposit SiO_2. To provide clue for this mechanism we proceed to test the growth of chemical gardens in HCl vapor. For this, the same set up system was used but the chamber was filled with fuming HCl (37%) and allowed to saturate with gaseous HCl. Then, the silicate solution was injected as previously, and the formation of chemical garden was successfully demonstrated (not shown). The XRD analysis of this chemobrionic structure showed the presence of amorphous SiO_2 and halite (Fig. 2 dark yellow diffractogram). The growth of chemical gardens in pure acidic atmospheres could be considered the complementary of the previously described growth of chemical gardens in only hydroxide solution.[4]

To this end, we investigated whether injection of 3 M sodium phosphate (pH 8.7) instead of silicate in the atmosphere of $TiCl_4$ could form chemical gardens. For a range of flow rates between 0.050 to 0.230 mL min^{-1}, we could not obtain any formation of a chemobrionic structure. Therefore, no titanium phosphate deposits were produced, further supporting the proposed mechanism of chemical garden formation, that is based on hydrolysis of $TiCl_4$. Also, no chemobrionic structures were obtained when injection of 3 M NaOH solution was carried out in an atmosphere of $TiCl_4$. These control experiments highlight the importance of silicates in the formation of these types of chemical gardens.

Then we analyzed the growth velocity of chemobrionic structures for different flows (Q) of the injected solution. When, the data were plotted in logarithmically scaled axes as previously,[4] a power law dependance where $v = kQ^{\alpha}$ was revealed. In this equation, the power law exponent α = 0.9003 (Fig. 3). No deviation from the power law is found for a range of Q between 0.050 mL min^{-1} and 0.280 mL min^{-1}. Previously deviations from the power law were ascertain on the effect of buoyancy at low Q.[4] Here, buoyancy is most likely not expected to participate in the growth of chemobrionic structures since their development is taking place in the direction of gravity and most importantly in gaseous phase. In accordance, the value of 0.9003 is close to 1. We have also tried to grow chemical garden by injecting silicate solution in a saturated $TiCl_4$ atmosphere against gravity, as conducted in usual chemical garden formation experiments. Nonetheless, for Q between 0.050 and 0.280 mL min^{-1} no growth was obtained. Instead, the chemobrionic structure was growing in the direction of gravity through creeping from the injection nozzle (Fig. S1, ESI†).

The chemobrionic structures were analyzed with scanning electron microscopy (SEM) to determine the microstructure. In addition, energy dispersive X-ray spectroscopy (EDS) was used to analyze the distribution of the main elements in the

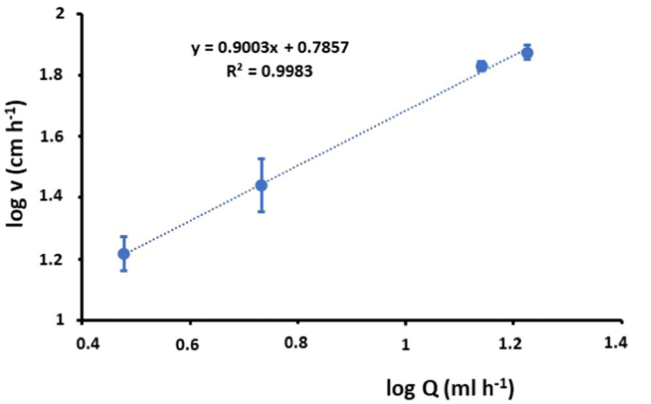

Fig. 3 Power law dependance of log(velocity of growth) *vs.* log(flow rate). The slope that corresponds to α in the equation $v = kQ^{\alpha}$ equals to 0.9003 ± 0.0394. The data shown were obtained with injection of 14% silicate solution in $TiCl_4$ atmosphere. The data represent mean ± standard deviation.

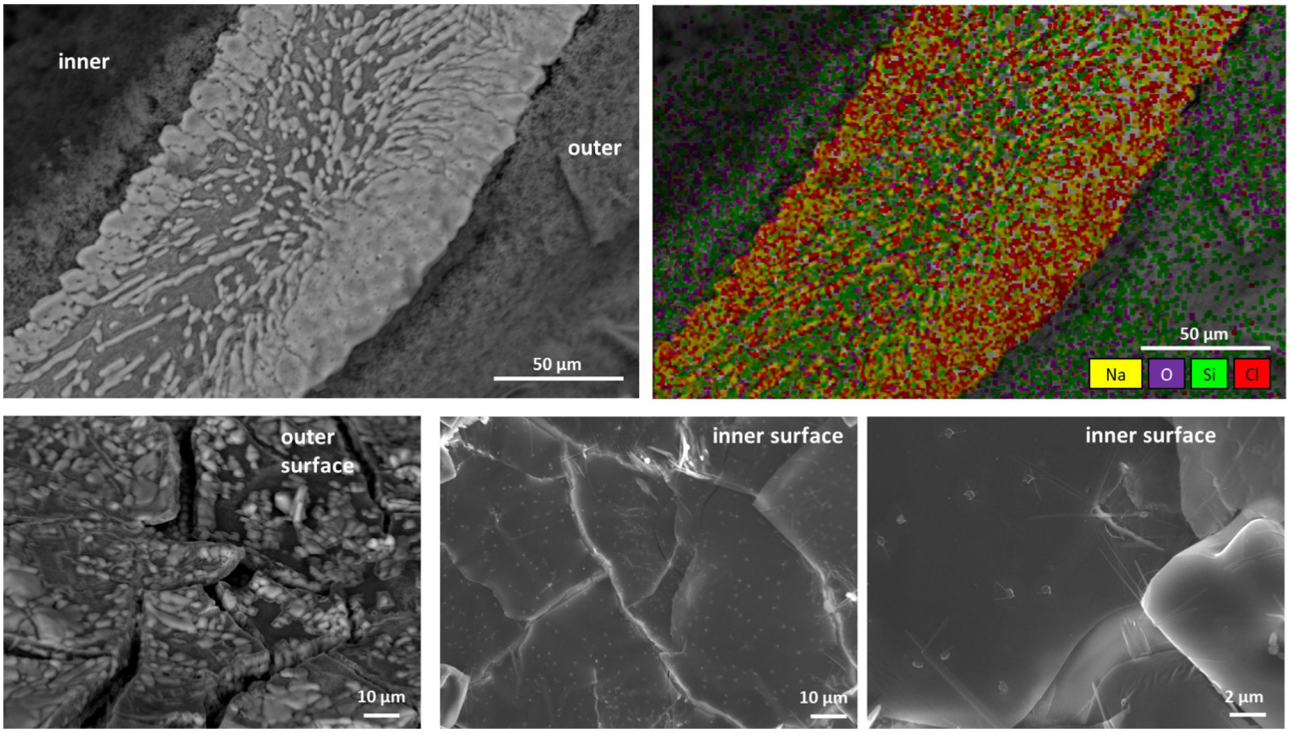

Fig. 4 Microscopic characterization of the chemobrionic structures grown in $TiCl_4$ atmosphere through injection of 14% silicate solution. On the upper left, a cross-section of the chemical garden is shown. On the upper right a map of the elemental analysis of the cross-section is shown. On the lower the structure of the outer and inner surface is shown. The images were obtained on FESEM-JSM-7610 FPlus (JEOL) equipped with an EDS detector (AZTEC ONE STD XACT) for the elemental analysis.

cross-section of the structure. For this, the samples were initially sputtered with carbon and then observed with a Field-Emission SEM equipped with an EDS detector. As show in Fig. 4, the exterior surface of the tube is composed to small sheets resembling tiles that are rough. On the contrary, the inner surface is exceptionally smooth as also revealed with higher magnification. In the cross-section, it appears that the structure of chemical gardens can be separated into three different layers. The area in the middle is mostly SiO_2, while it contains long stripes (shown in white) that are mainly NaCl. Further, the part of the region in the middle that is in contact with the inner and the outer surface also contains NaCl. More specifically, NaCl localizes with the white long stripes embedded in the SiO_2 (as shown in the chemical analysis map-yellow and red colors in Fig. 4). Thus, significant amounts of NaCl are enclosed in the chemobrionic structure providing an explanation on why NaCl did not wash away during the washing step. Notably, no titanium trace has been found which probably indicates that its amount is very low. In conclusion, the chemical composition of the material is amorphous silicon dioxide with small amounts of NaCl interspaced randomly within it. When, the material is grown in the $TiCl_4$ atmosphere, it is also decorated by small amounts of TiO_2.

The described chemical gardens are reminiscent of calthemites,[16,17] the calcite straws that grow on the roof of basements, under bridges and generally under manmade structures that use concrete. Under these conditions, water can penetrate through cracks in cement and cement-like materials and form an alkaline fluid that in turn, as it travels through cracks and exits the structure, encounters atmospheric CO_2, and generates stalactite-like hollow structures made from calcite.[16] Thus these experiments may be set the basis for the generation of the laboratory analogues of calthemites and related geochemical structures like the calthemites produced in rocked-filled dams.[17] The same set up can be used to delineate the mechanism of growth of soda straws. Finally, this method results in the generation of chemical gardens that may hold new applications in materials/biomaterials science. In this direction, silicon dioxide is considered a new bone substitute[18] and thus this study may provide an alternative scaffold with potential use in bone regeneration.

The authors would like to acknowledge the COST Action CA17120 Chemobrionics. We would like to thank Dimitrios Bikiaris (Department of Chemistry, Aristotle University of Thessaloniki, Greece) for XRD. We would also like to thank Eleni Pavlidou and Chrysanthi Papoulia for SEM and EDS analysis (Department of Physics, Aristotle University of Thessaloniki, Greece).

Conflicts of interest

There are no conflicts to declare.

Notes and references

1 J. R. Glauber, *Furni Novi Philosophici*, Johan Jansson, Amsterdam, 1646.

2 L. M. Barge, S. S. Cardoso, J. J. Cartwright, G. T. Cooper, L. Cronin, A. De Wit, I. J. Doloboff, B. Escribano, R. E. Goldstein, F. Haudin, D. E. Jones, A. L. Mackay, J. Maselko, J. J. Pagano, J. Pantaleone, M. J. Russell, C. I. Sain-Diaz, O. Steinbock, D. A. Stone, Y. Tanimoto and N. L. Thomas, *Chem. Rev.*, 2015, **115**, 8652–8703.
3 (*a*) G. Pampalakis, *Chem. – Eur. J.*, 2016, **22**, 6779–6782; (*b*) F. Bernini, E. Castellini, L. Sebastianelli, B. Bighi, C. I. Sainz-Díaz, A. Mucci, D. Malferrari, A. Ranieri, M. F. Brigatti and M. Borsari, *Chemsystemschem*, 2021, **3**, e200048; (*c*) R. Zahorán, P. Kumar, A. Juhász, D. Horváth and A. Tóth, *Soft Matter.*, 2022, **18**, 8157–8164.
4 B. C. Batista and O. Steinbock, *Chem. Commun.*, 2015, **51**, 12962–12965.
5 J. M. García-Ruiz, E. Nakouzi, E. Kotopoulou, L. Tamborrino and O. Steinbock, *Sci. Adv.*, 2017, **3**, e1602285.
6 J. H. E. Cartwright, J. M. García-Ruiz, M. L. Novella and F. Otálora, *J. Colloid Interface Sci.*, 2002, **256**, 351–359.
7 S. Thouvenel-Romans and O. Steinbock, *J. Am. Chem. Soc.*, 2003, **125**, 4338–4341.
8 L. M. Barge, Y. Abedian, I. J. Doloboff, J. E. Nuñez, M. J. Russell, R. D. Kidd and I. Kanik, *J. Vis. Exp.*, 2015, **105**, 53015.
9 S. S. S. Cardoso, J. H. E. Cartwright and C. I. Sainz-Díaz, *Icarus*, 2019, **319**, 337–348; G. Angelis, G. G. Kordopati, E. Zingkou, A. Karioti, G. Sotiropoulou and G. Pampalakis, *Chem. – Eur. J.*, 2021, **27**, 600–604.
10 D. A. Stone and R. E. Goldstein, *Proc. Natl. Acad. Sci. U. S. A.*, 2004, **101**, 11537–11541.
11 S. S. S. Cardoso, J. H. E. Cartwright, O. Steinbock, D. A. Stone and N. L. Thomas, *Struct. Chem.*, 2017, **28**, 33–37; D. D. Double and A. Hellawell, *Nature*, 1976, **261**, 486–488.
12 G. Angelis, D. N. Zayed, A. Karioti, D. Lazari, E. Kanata, T. Sklaviadis and G. Pampalakis, *Chem. – Eur. J.*, 2019, **25**, 12916–12919.
13 K. Punia, M. Bucaro, A. Mancuso, C. Cuttitta, A. Marsillo, A. Bykov, W. L'Amoreaux and K. S. Raja, *Langmuir*, 2016, **32**, 8748–8758.
14 E. A. B. Hughes, M. Chipara, T. J. Hall, R. L. Williams and L. M. Grover, *Biomater. Sci.*, 2020, **8**, 812–822.
15 B. Paul, R. Drysdale, H. Green, J. Woodhead, J. Hellstrom and R. Eberhand, *Int. J. Speleol.*, 2013, **42**, 155–160.
16 P. L. Broughton, *Environ. Earth Sci.*, 2020, **79**, 245.
17 K. Yoshimura, O. Watanabe and J. Miyake, *Appl. Geochem.*, 2023, **148**, 105488.
18 (*a*) J. L. Hass, E. M. Harrison, S. A. Wicher, N. Kapp, D. N. Mcllory and G. Arrizabalaga, *J. Nanobiotechnol.*, 2012, **10**, 6; (*b*) U. K. Roopavath, R. Soni, U. Mahanta and A. S. Deshpande, *RSC Adv.*, 2019, **9**, 23832–23842; (*c*) L. F. C. Lehman, M. S. Noronha, I. M. A. Diniz, R. M. F. da Costa e Silva, A. L. Andrade, L. F. de Sousa Lima, C. E. P. de Alcántara, R. Domingues, A. J. Ferreira, T. A. da Silva and R. A. Mesquita, *J. Tissue Eng. Regen. Med.*, 2019, **13**, 1651–1663.

